

We are IntechOpen, the world's leading publisher of Open Access books Built by scientists, for scientists

6,900

Open access books available

186,000

International authors and editors

200M

Downloads

Our authors are among the

154

Countries delivered to

TOP 1%

most cited scientists

12.2%

Contributors from top 500 universities



WEB OF SCIENCE™

Selection of our books indexed in the Book Citation Index
in Web of Science™ Core Collection (BKCI)

Interested in publishing with us?
Contact book.department@intechopen.com

Numbers displayed above are based on latest data collected.
For more information visit www.intechopen.com



Design of Passive UHF RFID Tag Antennas Using Metamaterial-Based Structures and Techniques

Benjamin D. Braaten¹ and Robert P. Scheeler²

¹North Dakota State University

²University of Colorado – Boulder
United States

1. Introduction

Metamaterials (Marques et al., 2008; Eleftheriades & Balmain, 2005; Herraiz-Martinez et al. 2009) are one of the many new technologies being adopted to improve the performance of radio frequency identification (RFID) systems (Finkenzeller, 2003; Stupf et al., 2007). In particular, metamaterial-based antenna designs are being used more frequently to improve the read range and reduce the size of passive UHF RFID tags. This chapter will introduce the concept of RFID systems and the relevant parameters for proper antenna design. Then, expressions for the phase constants, propagation constants and the characteristic (or Bloch) impedance of a wave propagating down an infinite transmission line (TL) will be derived. These expressions will then be used to introduce the concept of LH-propagation. Subsequently, the design of several metamaterial-based antennas for passive UHF RFID tags will be summarized followed by a section on the conclusion and future applications of metamaterial-based antennas to RFID systems.

2. An introduction to passive UHF RFID systems using the Friis transmission equation

The RFID system in Fig. 1 consists of a reader and several RFID tags in the space around the reader. A transmit and receive antenna is connected to the reader and each tag has a single antenna used for both transmitting and receiving. Digital circuitry that communicates with the reader is attached to the antenna on the RFID tag. This digital circuitry is often denoted as the passive IC on the RFID tag. To communicate with the tags, the reader sends out an electromagnetic field using the transmitting antenna. This electromagnetic field has power and timing information that will be used by the tag. If a tag is close enough to the reader, the tag will harvest some of the incoming energy from the electromagnetic field to power the digital circuitry in the passive IC. If it is appropriate, the passive IC will communicate with the reader using backscattered waves. By changing the input impedance of the passive IC connected to the tag antenna, the tag is able to create two different backscattered waves in the direction of the reader. One backscattered wave corresponds to a logic 0 and the other backscattered wave corresponds to a logic 1. By using timing information with the two

Source: Radio Frequency Identification Fundamentals and Applications, Design Methods and Solutions, Book edited by: Cristina Turcu, ISBN 978-953-7619-72-5, pp. 324, February 2010, INTECH, Croatia, downloaded from SCIYO.COM

backscattered waves, the tag is able to transmit a digital signal back to the reader. This backscattered wave with the digital information is then received by the receive antenna connected to the reader and processed.

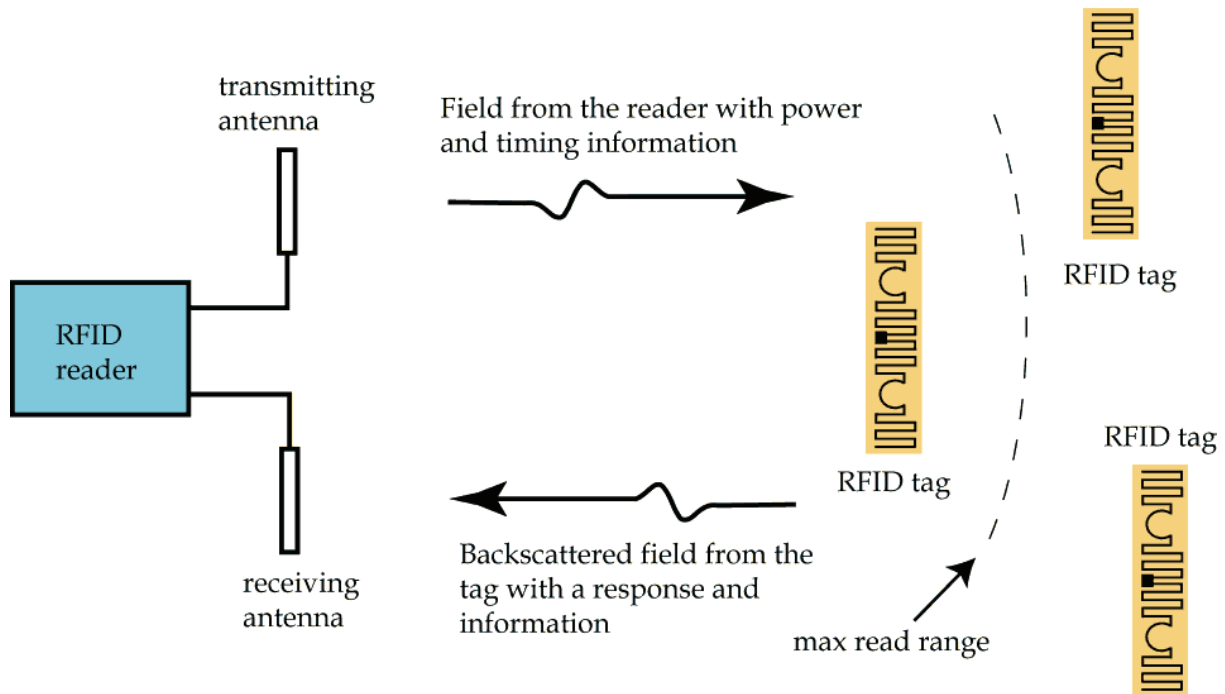


Fig. 1. Overview of a passive RFID system.

There are several different methods to describe the characteristics of a passive UHF RFID system (Braaten et al., 2006; Finkenzeller, 2003). The Friis transmission equation (Stutzman & Thiele, 1998) will be used here to show the relevant properties of an antenna on a RFID tag for achieving a maximum read range.

In general, the gain of the antennas, transmit power, frequency and sensitivity of the receiver determine the distance and rate at which a communication system can transfer digital information wirelessly. A convenient expression for describing the characteristics of such wireless systems is the Friis transmission equation (Stutzman & Thiele, 1998):

$$P_r = P_t \frac{G_r G_t \lambda^2}{(4\pi R)^2} q \quad (1)$$

where P_t is the transmitted power, P_r is the receive power, G_t is the gain of the transmitting antenna, G_r is the gain of the receiving antenna, λ is the free-space wavelength of the transmitting frequency, R is the distance between the antenna on the transmitter and the antenna on the receiver and q is the impedance mismatch factor ($0 \leq q \leq 1$) between the receiver and the receiving antenna. Equation (1) assumes a polarization match between the transmitting antenna and receiving antenna and that the receiving antenna is in the far-field of the transmitting antenna.

Equation (1) can be adopted to describe the performance of the RFID system on Fig. 1. In a RFID system, the transmitter is the reader and the receiver is the tag. The reader is connected to a transmitting antenna with a fixed gain and the tag has a receiving antenna with a fix gain. Rewriting (1) with a few substitutions results in the following expression:

$$P_{tg} = P_{rd} \frac{G_{rd} G_{tg} \lambda^2}{(4\pi R)^2} q \quad (2)$$

where P_{rd} is the power transmitted by the reader, P_{tg} is the power received by the passive tag, G_{rd} is the gain of the transmitting antenna on the reader, G_{tg} is the gain of the space-filling antenna on the tag, λ is the free-space wavelength of the transmitting frequency by the reader, R is the distance between the antenna on the reader and the antenna on the tag and q is the impedance mismatch factor ($0 \leq q \leq 1$) between the passive IC and the antenna on the tag. Next, solving for R in (2) results in the following expression (Braaten et al., 2008; Rao et al., 2005):

$$R = \frac{\lambda}{4\pi} \sqrt{\frac{q G_{rd} G_{tg} P_{rd}}{P_{tg}}}. \quad (3)$$

Equation (3) represents the distance needed to observe a particular value of P_{tg} for some fixed transmit power by the reader, fixed transmit gain and a fixed gain for the antenna on the RFID tag. Therefore, if the threshold power required to activate the passive IC and communicate with the reader is denoted as P_{th} , then a maximum read range r_{max} can be derived from (3) with a simple substitution:

$$r_{max} = \frac{\lambda}{4\pi} \sqrt{\frac{q G_{rd} G_{tg} P_{rd}}{P_{th}}}. \quad (4)$$

Equation (4) is a very useful expression and often common method for predicting the max read range of a passive RFID tag (Vaselaar, 2008; Rao et al., 2007). Typically, in a passive UHF RFID system it is very desirable to achieve the longest possible read range. Usually, P_{th} is fixed by the manufacture of the passive IC, while P_{rd} , G_{rd} and λ are fixed by the laws of the country the RFID system may be operating in. This leaves G_{tg} and q available for the design of the antenna on the passive RFID tag to maximize the read range.

3. Introduction to Left-handed propagation

Many different methods exist for improving the read range and reducing the size of a passive RFID tag. One such method is to incorporate metamaterial concepts into the design of the antenna on the RFID tag (Braaten et al., 2009a). In the next section, the concept of metamaterials is introduced by deriving expressions for the propagation constant, phase velocity and Bloch impedance of a LH-wave propagating down an infinite transmission line (Gil et al., 2007; Ryu et al., 2008). But first, a few comments on the terminology of LH-propagation are in order.

The terms RH- and LH-propagation refers to the direction of the wave vector k . In a traditional RH-TL, the electric field is curled into the magnetic field using the right hand. The field components for the RH-case are shown in Fig. 2 (a). After the curl, the thumb is pointing in the direction of the Poynting vector S and k . In a LH-TL, k is pointing in the opposite direction as S . This case is shown in Fig. 2 (b). This then requires curling the electric field into the magnetic field using the left hand. Then the direction of the thumb is pointing in the direction of k but in the opposite direction as S . Notice in both cases that S is always pointing in the same direction which indicates that the power is always flowing in the same direction (i.e., power is flowing to the load). This is the case regardless if the TL supports RH- or LH-propagation.

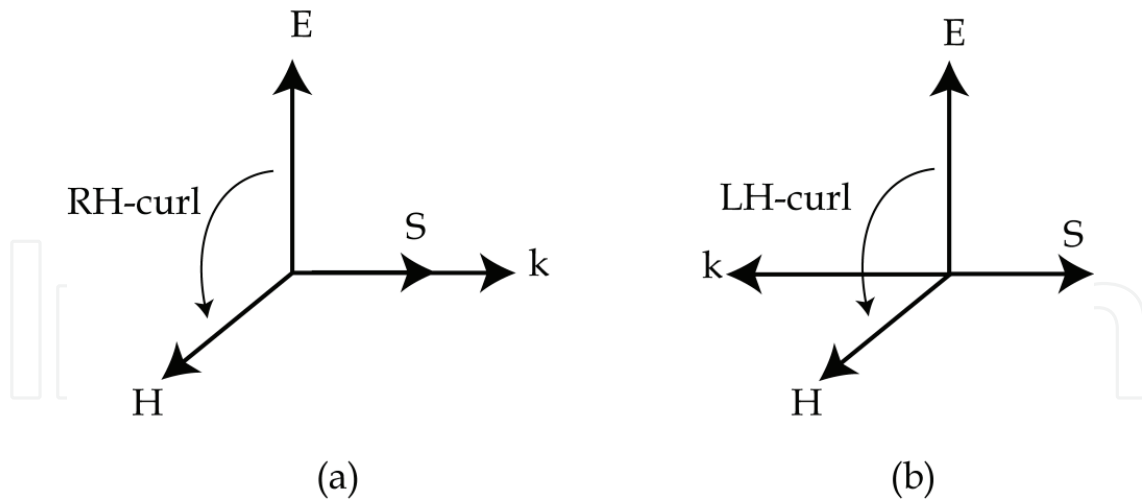


Fig. 2. (a) RH-propagation terminology; (b) LH-propagation terminology.

3.1 Deriving the Bloch impedance from an infinite periodic structure with loads that are in parallel.

First consider the equivalent circuit of the infinite TL in Fig. 3. Fig. 3 shows a periodically loaded TL with admittances jb . Using ABCD matrices (Pozar, 2005), the voltage and current at either side of the n^{th} unit cell is

$$\begin{bmatrix} V_n \\ I_n \end{bmatrix} = \begin{bmatrix} A & B \\ C & D \end{bmatrix} \begin{bmatrix} V_{n+1} \\ I_{n+1} \end{bmatrix}. \tag{5}$$

Then using Table 4.1 in Pozar (2005), the normalized form of the ABCD matrix can be written as:

$$\begin{aligned} \begin{bmatrix} A & B \\ C & D \end{bmatrix} &= \begin{bmatrix} \cos \frac{\theta}{2} & j \sin \frac{\theta}{2} \\ j \sin \frac{\theta}{2} & \cos \frac{\theta}{2} \end{bmatrix} \begin{bmatrix} 1 & 0 \\ jb & 1 \end{bmatrix} \begin{bmatrix} \cos \frac{\theta}{2} & j \sin \frac{\theta}{2} \\ j \sin \frac{\theta}{2} & \cos \frac{\theta}{2} \end{bmatrix} \\ &= \begin{bmatrix} \cos \theta - \frac{b}{2} \sin \theta & j \left(\sin \theta + \frac{b}{2} \cos \theta - \frac{b}{2} \right) \\ j \left(\sin \theta + \frac{b}{2} \cos \theta + \frac{b}{2} \right) & \cos \theta - \frac{b}{2} \sin \theta \end{bmatrix} \end{aligned} \tag{6}$$

where $\theta = kd$ and k is the propagation constant of the unloaded line. Next, the voltage and current for a wave propagating in the $+z$ -direction can be written as:

$$V(z) = V(0)e^{-\gamma z} \tag{7}$$

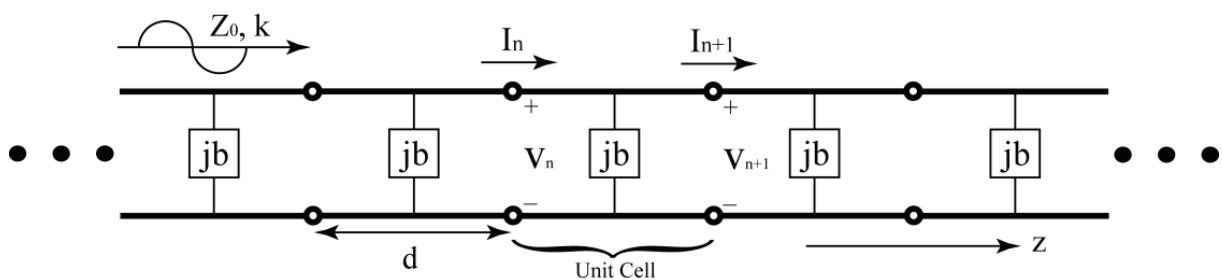


Fig. 3. Infinite periodic transmission line with parallel loads.

and

$$I(z) = I(0)e^{-\gamma z}. \quad (8)$$

Since the structure in Fig. 3 is infinitely long, V and I at the $(n + 1)^{th}$ terminal differ from the n^{th} terminal by a factor of $e^{-\gamma d}$, where d is the length of each unit cell along the TL. This then gives

$$V_{n+1} = V_n e^{-\gamma d} \quad (9)$$

and

$$I_{n+1} = I_n e^{-\gamma d}. \quad (10)$$

Solving for the voltage and current at the n^{th} terminal gives:

$$V_n = V_{n+1} e^{\gamma d} \quad (11)$$

and

$$I_n = I_{n+1} e^{\gamma d}. \quad (12)$$

Thus,

$$\begin{bmatrix} V_n \\ I_n \end{bmatrix} = \begin{bmatrix} A & B \\ C & D \end{bmatrix} \begin{bmatrix} V_{n+1} \\ I_{n+1} \end{bmatrix} = \begin{bmatrix} V_{n+1} e^{\gamma d} \\ I_{n+1} e^{\gamma d} \end{bmatrix}. \quad (13)$$

Subtracting the matrix on the right of (13) from the middle matrices in (13) gives:

$$\begin{bmatrix} A - e^{\gamma d} & B \\ C & D - e^{\gamma d} \end{bmatrix} \begin{bmatrix} V_{n+1} \\ I_{n+1} \end{bmatrix} = 0. \quad (14)$$

Next, the determinant of (14) must vanish for a nontrivial solution (Pozar, 2005), or

$$(A - e^{\gamma d})(D - e^{\gamma d}) - BC = AD - De^{\gamma d} - Ae^{\gamma d} + e^{2\gamma d} - BC = 0. \quad (15)$$

Factoring (15) gives

$$e^{2\gamma d} - e^{\gamma d}(A + D) + 1 = 0. \quad (16)$$

Since (6) is a normalized matrix, $AD - BC = 1$. This reduces (16) to

$$A + D = e^{-\gamma d} + e^{\gamma d}. \quad (17)$$

Then using $\cosh(\gamma d) = \frac{e^{-\gamma d} + e^{\gamma d}}{2}$ results in

$$\cosh(\gamma d) = \frac{A+D}{2} \quad (18)$$

where A and D are taken from the matrix in (6). Since $\gamma = \alpha + j\beta$, the following expression can also be written

$$\cosh(\gamma d) = \cos\theta - \frac{b}{2}\sin\theta. \quad (19)$$

Notice that (19) is written in terms of the propagation constants and the length of the TL. Next, an expression for the characteristic impedance for the wave along the TL is derived. This impedance is sometimes called the Bloch impedance Z_B . To derive Z_B , first start with

$$Z_B = Z_0 \frac{V_{n+1}}{I_{n+1}} \quad (20)$$

which is the characteristic impedance of the n^{th} unit cell in Fig. 3. Next, solving for V_{n+1} in (13) gives:

$$V_{n+1} = \frac{-BI_{n+1}}{A - e^{\gamma d}}. \quad (21)$$

Substituting (21) into (20) results in

$$Z_B = \frac{-BZ_0}{A - e^{\gamma d}}. \quad (22)$$

Next, solving for the root in (16) results in the following expression for $e^{\gamma d}$:

$$e^{\gamma d} = \frac{(A+D) \pm \sqrt{(A+D)^2 - 4}}{2} \quad (23)$$

Next, substituting (23) into (22) gives

$$Z_B^{\pm} = \frac{-2BZ_0}{2A - A - D \mp \sqrt{(A+D)^2 - 4}}. \quad (24)$$

For reciprocal networks, $A = D$. Thus, (24) reduces to

$$Z_B^{\pm} = \frac{\pm BZ_0}{A^2 - 1}. \quad (25)$$

Equation (25) is the characteristic impedance, or Bloch impedance, of the infinite periodic TL in Fig. 3. Therefore, once the admittance jb is known, A and B can be taken from (6) to evaluate the Bloch impedance along the TL. In the next section, derivations for a similar expression to (25) are presented for a general infinite periodic TL.

3.2 Deriving the Bloch impedance from an infinite periodic structure with loads that are in series and parallel.

Again, the first step in the derivation of the Bloch impedance for the the infinite TL in Fig. 4 is to write the ABCD matrix. Using Table 4.1 in Pozar (2005), the following expressions can be written for A , B , C and D :

$$A = 1 + \frac{Z_s}{Z_p} \quad (26)$$

$$B = Z_s \left(2 + \frac{Z_s}{Z_p} \right) \quad (27)$$

$$C = \frac{1}{Z_p} \quad (28)$$

$$D = 1 + \frac{Z_s}{Z_p} = A. \quad (29)$$

Also, note again that $AD - BC = 1$ and that the voltage and current for a wave propagating in the $+z$ -direction can be written as:

$$V(z) = V(0)e^{-\gamma z} \quad (30)$$

and

$$I(z) = I(0)e^{-\gamma z}. \quad (31)$$

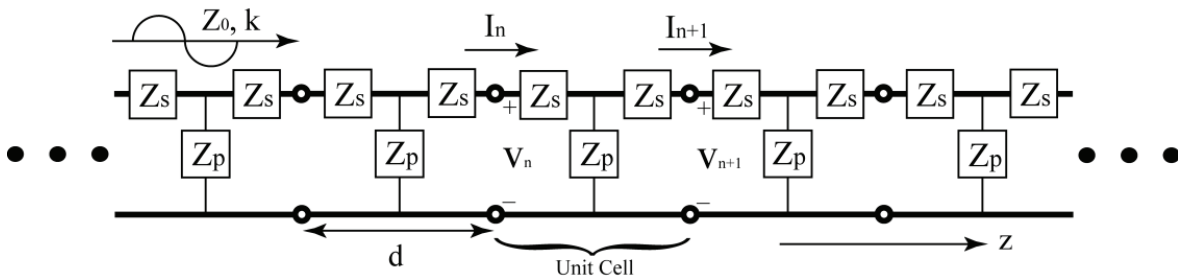


Fig. 4. Generalized infinite periodic transmission line with series and parallel loads.

Since the structure in Fig. 4 is infinitely long, V and I at the $(n + 1)^{th}$ terminal differ from the n^{th} terminal by a factor of $e^{-\gamma d}$ where d is the length of each unit cell along the TL. This then gives

$$V_{n+1} = V_n e^{-\gamma d} \quad (32)$$

and

$$I_{n+1} = I_n e^{-\gamma d}. \quad (33)$$

Solving for the voltage and current at the n^{th} terminal gives:

$$V_n = V_{n+1} e^{\gamma d} \quad (34)$$

and

$$I_n = I_{n+1} e^{\gamma d}. \quad (35)$$

Thus,

$$\begin{bmatrix} V_n \\ I_n \end{bmatrix} = \begin{bmatrix} A & B \\ C & D \end{bmatrix} \begin{bmatrix} V_{n+1} \\ I_{n+1} \end{bmatrix} = \begin{bmatrix} V_{n+1} e^{\gamma d} \\ I_{n+1} e^{\gamma d} \end{bmatrix}. \quad (36)$$

Subtracting the matrix on the right of (36) from the middle matrices in (36) gives:

$$\begin{bmatrix} A - e^{\gamma d} & B \\ C & D - e^{\gamma d} \end{bmatrix} \begin{bmatrix} V_{n+1} \\ I_{n+1} \end{bmatrix} = 0. \quad (37)$$

Next, the determinant of (37) must vanish for a nontrivial solution (Pozar, 2005), or

$$(A - e^{\gamma d})(D - e^{\gamma d}) - BC = AD - De^{\gamma d} - Ae^{\gamma d} + e^{2\gamma d} - BC = 0. \quad (38)$$

Factoring (38) gives

$$e^{2\gamma d} - e^{\gamma d}(A + D) + 1 = 0. \quad (39)$$

Since $AD - BC = 1$, (39) reduces to

$$A + D = e^{-\gamma d} + e^{\gamma d}. \quad (40)$$

Then using $\cosh(\gamma d) = \frac{e^{-\gamma d} + e^{\gamma d}}{2}$ results in

$$\cosh(\gamma d) = \frac{A+D}{2} = \cosh(\alpha d) \cos(\beta d) + j \sinh(\alpha d) \sin(\beta d) = \frac{1 + \frac{Z_s}{Z_p} + 1 + \frac{Z_s}{Z_p}}{2} \quad (41)$$

where A and D are taken from (26) and (29), respectively, and the trigonometric expressions are from the normalized matrix (6). This implies

$$\cosh(\alpha d) \cos(\beta d) + j \sinh(\alpha d) \sin(\beta d) = 1 + \frac{Z_s}{Z_p}. \quad (42)$$

Now, for the propagation mode we have $\alpha = 0$ and $\beta \neq 0$. Substituting α and β into (42) gives

$$\cosh(\beta d) = 1 + \frac{Z_s}{Z_p}. \quad (43)$$

Now for the Bloch impedance,

$$Z_B = Z_0 \frac{V_{n+1}}{I_{n+1}}. \quad (44)$$

Substituting (37) into (44) and solving for Z_B gives

$$Z_B = \frac{-B Z_0}{A - e^{\gamma d}}. \quad (45)$$

Next, solving for the root in (39) results in the following expression for $e^{\gamma d}$:

$$e^{\gamma d} = \frac{(A+D) \pm \sqrt{(A+D)^2 - 4}}{2} \quad (46)$$

Substituting (46) into (45), using $A = D$ and factoring results in the following expression for Z_B (Marques et al., 2008):

$$Z_B = \sqrt{Z_s(Z_s + 2Z_p)} \quad (47)$$

which is an expression for the Bloch impedance in terms of the series and parallel loads along the TL. Next, Z_s and Z_p will be defined in a manner to support both RH- and LH-propagation. Expressions will also be derived for Z_B in both instances.

First consider the RH-TL. In a RH-TL the series impedance is $Z_s = j\omega L/2$ and the parallel (or shunt) impedance is $Z_p = -j/\omega C$ in Fig. 4 (Marques et al., 2008; Eleftheriades & Balmain, 2005). This then reduces (43) to

$$\cosh(\beta_R d) = 1 + \frac{\omega^2 LC}{2}. \quad (48)$$

Note that the subscript R will be added to the variables to denote the RH-propagation. Similarly, a subscript L will be added to the variables to denote LH-propagation. Also, for the Bloch impedance,

$$Z_{BR} = \sqrt{Z_s(Z_s + 2Z_p)} = \sqrt{\frac{L}{C} \left(1 - \frac{\omega^2}{\omega_{CR}^2}\right)} \quad (49)$$

where $\omega_{CR}^2 = \left(\frac{2}{\sqrt{LC}}\right)^2$.

Next, in a LH-TL the series impedance is $Z_s = -j/2\omega C$ and the parallel (or shunt) impedance is $Z_p = j\omega L$ in Fig. 4 (Marques et al., 2008; Eleftheriades & Balmain, 2005). This then reduces (43) to

$$\cosh(\beta_L d) = 1 + \frac{1}{2LC\omega^2}. \quad (50)$$

Similarly for the Bloch impedance,

$$Z_{BL} = \sqrt{\frac{L}{C} \left(1 - \frac{\omega_{CL}^2}{\omega^2}\right)} \quad (51)$$

where $\omega_{CL}^2 = \left(\frac{2}{\sqrt{LC}}\right)^2$.

For the previous analysis it was assumed that $\lambda_d \gg d$ where λ_d is the internal wavelength and d is the segment length in Fig. 4. To ensure this inequality, the segment length d must be reduced. This translates to smaller values of L and C . Doing so increases the cutoff frequency ω_{CR} , thus the following expressions are only valid for frequencies that satisfy the inequality $\omega \ll \omega_{CR}$. This implies that $\frac{\omega}{\omega_{CR}} \ll 1$. This inequality simplifies (49) to

$$Z_{BR} \approx \sqrt{\frac{L}{C} (1 - 0)} = \sqrt{\frac{L}{C}}. \quad (52)$$

Also, for the LH-TL, (51) reduces to

$$Z_{BL} = \sqrt{\frac{L}{C} (1 - 0)} = Z_{BR} \quad (53)$$

because $\omega \gg \frac{\omega_{LC}^2}{\omega^2} \approx 0$.

The previous steps illustrate the process of deriving the Bloch impedance values for a RH- and LH-TL. In the next section, the derivation of the expressions for the propagation constants and phase velocities along a RH- and LH-TL will be presented.

3.3 Deriving the propagation constants and phase velocity expressions from an infinite periodic structure with loads that are in series and parallel.

First, taking the Taylor series expansion of (48) and truncating after the second term gives

$$\cos(\beta_R d) \approx 1 - \frac{(\beta_R d)^2}{2!} = 1 - \frac{\omega^2 LC}{2}. \quad (54)$$

Solving for the phase constant in (54) gives

$$\beta_R d = \omega\sqrt{LC}. \quad (55)$$

Then for the phase $V_{\phi R}$ and group V_{gR} velocity,

$$V_{\phi R} = \frac{\omega}{\beta_R} = \frac{d}{\sqrt{LC}} > 0 \quad (56)$$

and

$$V_{gR} = \left(\frac{\partial \beta_R}{\partial \omega}\right)^{-1} = V_{\phi R} > 0. \quad (57)$$

Next, using the Taylor series expansion of (50) and truncating after the second term gives

$$\cos(\beta_L d) \approx 1 - \frac{(\beta_L d)^2}{2!} = 1 - \frac{1}{2\omega^2 LC}. \quad (58)$$

Then solving for the phase constant in (58) and choosing the negative sign gives

$$\beta_L d = -\frac{1}{\omega\sqrt{LC}}. \quad (59)$$

Then for the phase $V_{\phi L}$ and group V_{gL} velocity,

$$V_{\phi L} = \frac{\omega}{\beta_L} = -\omega^2 d \sqrt{LC} < 0 \quad (60)$$

and

$$V_{gL} = \left(\frac{\partial \beta_L}{\partial \omega}\right)^{-1} = -V_{\phi L} > 0. \quad (61)$$

Note the inequalities in (60) and (61). In particular, notice the sign change in the phase velocity, but the group velocities remain positive. Looking at the summary in Table 1, it is clear which expressions in the LH-TL change sign for the LH-propagation. The RH-wave has a positive phase constant and phase velocity while a LH-wave have a negative phase constant and phase velocity. Both LH- and RH-waves have the same Bloch impedance (i.e., characteristic impedance) and positive group velocity. The sign of the group velocities were chosen to be both positive, which was done to agree with the definition of power flow (it is assumed that power flows from the source on the left to the load on the right of the TL in Fig. 4). Then in both instances, the group velocity is delivering power in the correct direction.

RH-TL	LH-TL
$Z_{BR} = \sqrt{\frac{L}{C}}$	$Z_{BL} = Z_{BR}$
$\beta_R d = \omega\sqrt{LC} > 0$	$\beta_L d = -\frac{1}{\omega\sqrt{LC}} < 0$
$V_{\phi R} = \frac{d}{\sqrt{LC}} > 0$	$V_{\phi L} = -\omega^2 d \sqrt{LC} < 0$
$V_{gR} = V_{\phi R} > 0.$	$V_{gL} = -V_{\phi L} > 0.$

Table 1. Summary of the derived RH- and LH-TL properties.

3.4 Dispersion diagrams for an infinite periodic structure with loads that are in series and parallel.

In this section the dispersion diagrams for the RH- and LH-TL are plotted. From Table 1, the propagation constants along a RH- and LH-TL are

$$\beta_R d = \omega\sqrt{LC} > 0 \quad (62)$$

and

$$\beta_L d = -\frac{1}{\omega\sqrt{LC}} < 0. \quad (63)$$

Solving for ω in (62) and (63) gives

$$\omega = \frac{\beta_R d}{\sqrt{LC}} \quad (64)$$

and

$$\omega = -\frac{1}{\beta_L d \sqrt{LC}}. \quad (65)$$

Plotting (64) and (65) results in the dispersion diagrams shown in Fig. 5 (normalized).

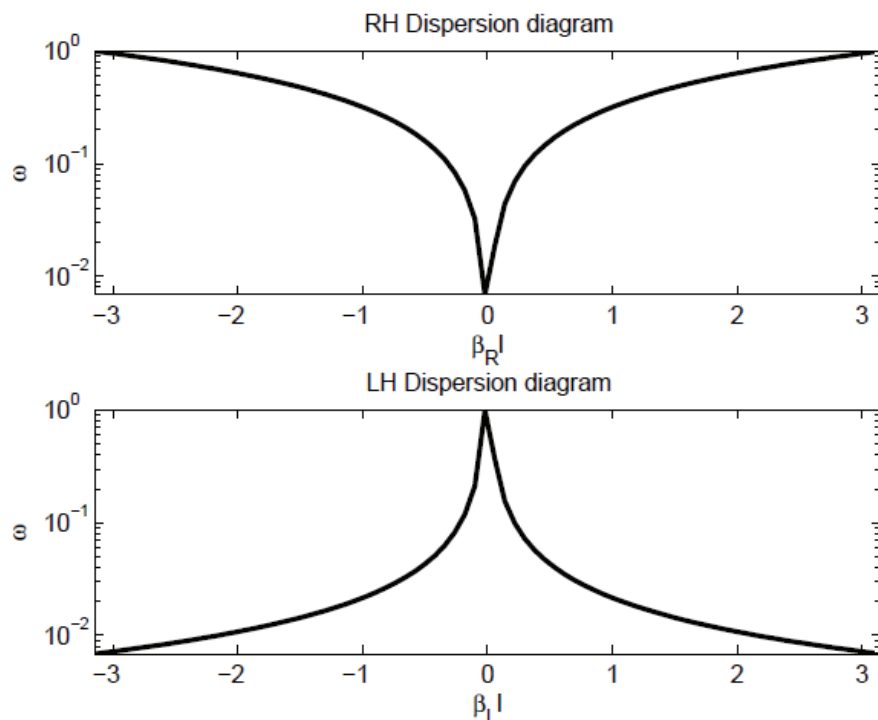


Fig. 5. RH- and LH-TL dispersion diagrams.

4. Metamaterial-based antennas for passive UHF RFID tags

As mentioned in the previous sections, one of the main advantages of using metamaterial-based elements in the design of antennas is that the resulting antenna is much smaller than traditional printed antennas (Lee et al, 2005; Lee et al., 2006; Abdalla et al., 2009; Iizuka & Hall, 2007). In this section, several of these ideas have been adopted for use on passive RFID tags. Particularly, metamaterial-based elements (Ali & Hu, 2008; Ghadarghadr et al., 2008) have been incorporated into the design of printed antennas on a single ungrounded dielectric. The first design shown in the next section uses deformed-omega elements (Mishra et al., 2008) to introduce a series inductance to the port of the antenna that causes the antenna to resonate at a much lower frequency (Braaten et al., 2009a). The second design

involves using coplanar waveguide elements (CPW) to reduce the overall size of a meander-line antenna. In particular, series connected CPW inductors and capacitors found in CPW filters (Mao et al., 2007) are used to periodically load a meander-line antenna. The result is a much smaller meander-line antenna with a lower resonant frequency (Braaten et al., 2009b). Finally, the third design uses two split-ring resonators (Marques et al., 2008; Eleftheriades & Balmain, 2005) instead of a meander-line antenna to form a dipole. This type of dipole is useful for RFID tags because the input impedance is inductive above the resonant frequency.

4.1 The Meander-line antenna

The printed meander-line antenna shown in Fig. 6 (a) is very useful for achieving resonance in a very small area. This makes the meander-line antenna very popular for integration on passive UHF RFID tags (Marrocco, 2003; Rao et al., 2005). It is often desirable to describe an antenna using an equivalent circuit. To do this, first consider the meander-line section in Fig. 6 (b). Each meander-line section can be modeled as a parallel connected equivalent capacitance C_m and equivalent inductance L_m (Bancroft, 2006). The equivalent capacitance exists between the vertical segments of each meander-line section and the self-inductance is created by the horizontal segments of each meander-line section. Thus, each pole of the meander-line dipole is made up of several series connected parallel $L_m C_m$ sections. In order for the meander-line antenna to resonate, it is important to maximize the section inductance L_m .

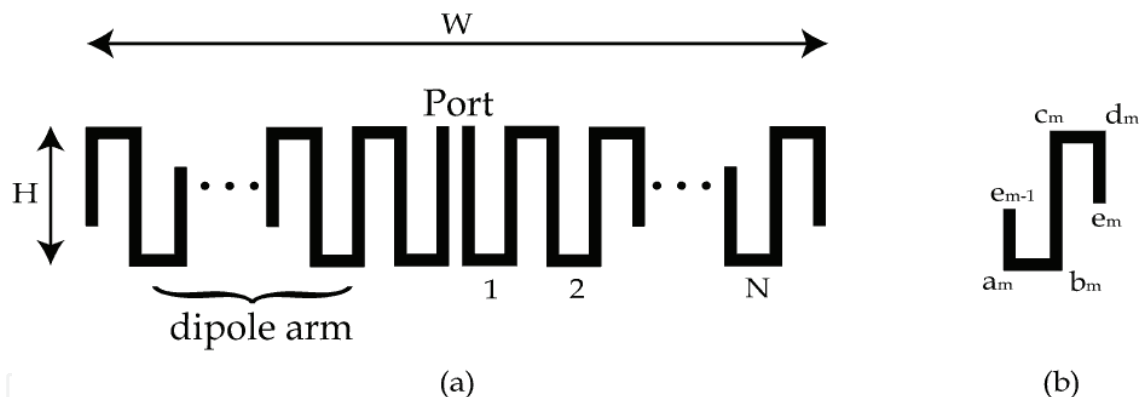


Fig. 6. (a) Meander-line antenna with N -elements on each arm; (b) the m^{th} meander-line section.

4.2 Meander-line antenna using deformed-omega elements

One way to improve the inductance of each section is to substitute the deformed-omega element shown in Fig. 7 (a) in for several of the meander-line sections (Braaten et al., 2009a). This added inductance will cause the meander-line antenna to resonate at a much lower frequency. This allows a designer to reduce the overall size of the meander-line antenna. The inductance of each deformed-omega element can be approximated as (Braaten et al., 2009a):

$$Z_a \approx \frac{1}{2} j \omega \mu_0 a \left[\ln \left(\frac{8a}{p} \right) - 2 \right] \Omega \quad (66)$$

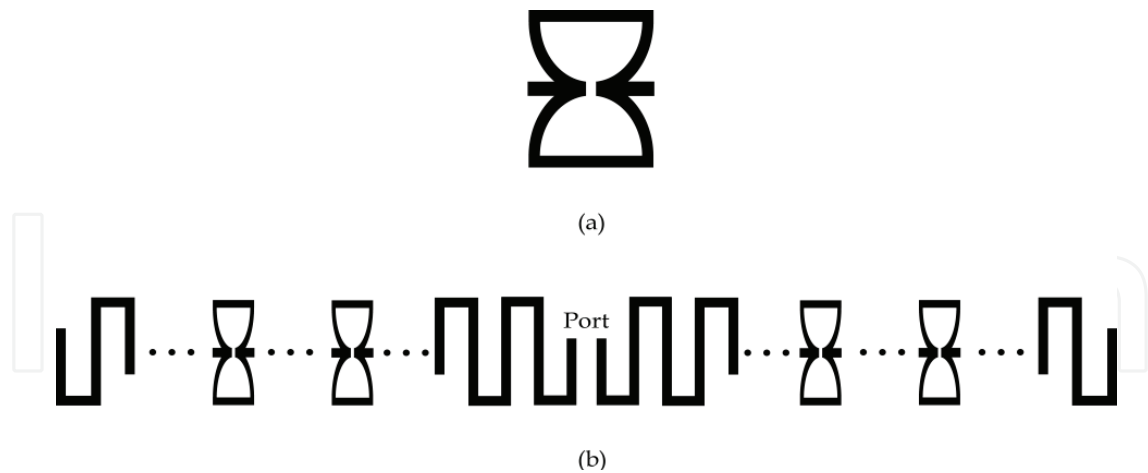


Fig. 7. (a) Deformed-omega element; (b) meander-line antenna with series connected deformed-omega elements.

where a is the width of the individual deformed-omega element and p is the trace width. Braaten et al. (2009a) has shown that the overall size of a meander-line antenna can be significantly reduced by introducing deformed-omega elements into the design. The prototype tag presented by Braaten et al. (2009a) is printed on FR-4 with a thickness of .787 mm. The overall size of the tag is 42.2 mm wide and 18.8 mm high and has a read range of 4.5 m. An image of the RFID tag is shown in Fig. 8. The size of the passive tag is being compared to a previous meander-line design by the same authors (Braaten et al., 2008).

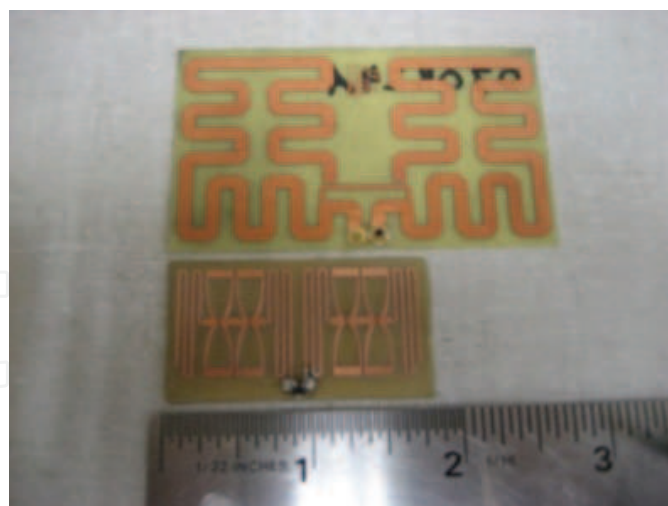


Fig. 8. A passive RFID tag with deformed-omega elements used in the antenna design being compared to the size of a previous meander-line design.

4.3 Meander-line antenna periodically loaded with right/left-handed CPW-LC loads

There are other methods to introduce inductance or capacitance to the equivalent circuit of each meander-line section. One method is to periodically load each meander-line section

with a series connected inductance (L) and capacitance (C) (Braaten et al., 2009b). It is often desirable to have the tag antenna on a single conducting layer. Thus, a CPW structure is needed to introduce the series L and C (Mao et al., 2007). An image of the series connected CPW-LC is shown in Fig. 9 (a). The load consists of an interdigitated capacitor connected to a conducting loop that introduces inductance. One method of periodically loading the meander-line antenna is shown in Fig. 9 (b). Periodic CPW-LC loads could also be introduced to the bottom of the meander-line antenna (Fig. 10).

Prototype designs using this method to load a meander-line antenna (Braaten et al. 2009b) have shown that the introduction of the periodic CPW LC-loads along the meander-line antenna reduces the overall size of the meander-line antenna by 18%. The prototype tag by Braaten et al. (2009b) was printed on 1.36 mm of FR-4 and had a max read range of 4.87 m. The overall size of the prototype tag was 14.81 mm high by 47.13 mm wide.

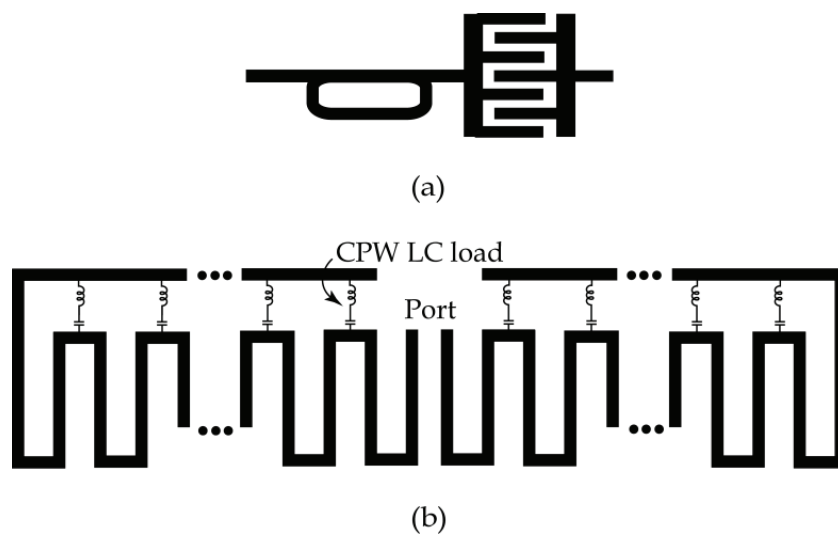


Fig. 9. (a) Series connected CPW-LC loads; (b) meander-line antenna periodically loaded with series connected LC loads

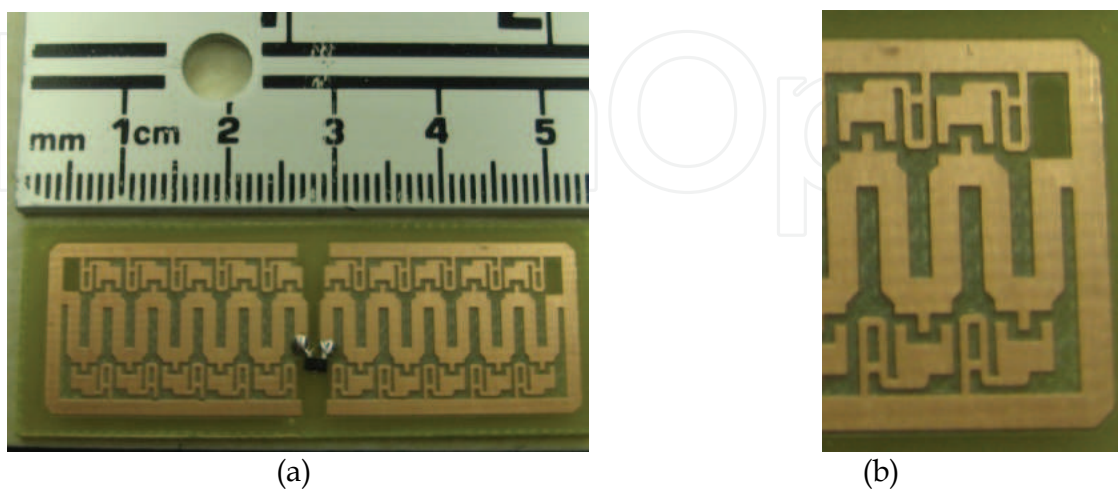


Fig. 10. (a) A meander-line antenna periodically loaded on the top and bottom with CPW-LC elements; (b) closer image of the CPW-LC loads.

4.4 Dipole antenna designed with split-ring resonators

The design of an antenna on a RFID tag does not always have to involve a meander-line antenna. As long as the antenna can be designed with an input impedance that is inductive, is compact in size and has a usable gain, then other elements may work. One element that can be used is the split-ring resonator (SRR) (Eleftheriates & Balmain, 2005) shown in Fig. 11. The equivalent circuit of a SRR is the same as each meander-line section shown in Fig. 6 (b). The particularly useful characteristic of a SRR is that this element is inductive above resonance (Dacuna & Pous, 2007). Therefore, a dipole could be made using two SRR as long as the dipole is driven above the resonance frequency.

Prototype RFID tags have been manufactured using a single SRR (Dacuna & Pous, 2007) and two SRRs (Braaten et al., 2009a) as a dipole. In both cases, the SRR were driven above resonance to achieve an inductive input impedance. Max read ranges of 6.5 m have been reported (Dacuna & Pous, 2007).

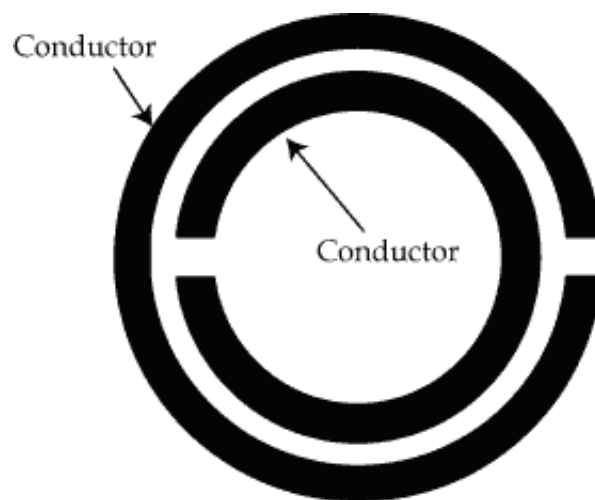


Fig. 11. Split-ring resonator element.

5. Conclusion

The first topic in this chapter was an introduction to RFID systems. This was followed immediately with a discussion on metamaterials and LH-propagation. Expressions for the propagation constants, phase velocity and Bloch impedance were derived and discussed. Next, several metamaterial-based antenna designs for passive RFID tags were presented. The designs offered showed that by incorporating elements found in metamaterials in the design of the antenna on a RFID tag, the antenna could be made to resonate at a much smaller dimension. The result is a compact passive RFID tag with very useful max read range values.

6. Future work

One common characteristic is shared among every antenna design in this chapter. Every design is based around an antenna with RH-propagation. An area that could be investigated

would be to achieve LH-propagation along a RFID antenna on a passive RFID tag. An antenna that achieves LH-propagation may have the added advantage of being much smaller than traditional meander-line antennas but many questions on the far-field characteristics (i.e., backscattering properties) of the antenna still need to be answered.

7. References

- Abdalla, M. A. Y.; Phang, K. & Eleftheriades, G. V., "A planar electronically steerable patch array using tunable PRI/NRI phase shifters," *IEEE Transactions on Microwave Theory and Techniques*, vol. 57, no. 3, pp. 531-541, March, 2009.
- Ali, A. & Hu, Z., "Metamaterial resonator based wave propagation notch for ultrawideband filter applications," *IEEE Antennas and Wireless Propagation Letters*, vol. 7, pp. 210-212, 2008.
- Bancroft, R. (2006). *Microstrip and Printed Antenna Design*, Scitech Publishing, Inc., Raleigh, North Carolina.
- Braaten, B.D.; Feng, Y. & Nelson, R.M., "High-frequency RFID tags: an analytical and numerical approach for determining the induced currents and scattered fields," *IEEE International Symposium on Electromagnetic Compatibility*, pp. 58-62, August 2006, Portland, OR.
- Braaten, B. D.; Owen, G. J.; Vaselaar, D.; Nelson, R. M.; Bauer-Reich, C.; Glower, J.; Morlock, B.; Reich, M.; & Reinholz, A., "A printed Rampart-line antenna with a dielectric superstrate for UHF RFID applications," in *Proceedings of the IEEE International Conference on RFID*, pp. 74-80, April, 2008, Las Vegas, NV.
- Braaten, B. D.; Scheeler, R. P.; Reich, M.; Nelson, R. M.; Bauer-Reich, C.; Glower, J. & Owen, G. J., "Compact metamaterial-based UHF RFID antennas: deformed omega and split-ring resonator structures," *Accepted for publication in the ACES Special Journal Issue on Computational and Experimental Techniques for RFID Systems and Applications*, 2009a.
- Braaten, B. D.; Reich, M. & Glower, J., "A compact meander-line UHF RFID tag antenna loaded with elements found in right/left-handed coplanar waveguide structures," *Submitted for review in the IEEE Antennas and Wireless Propagation Letters*, 2009b.
- Dacuna, J. & Pous, R. "Miniaturized UHF tags based on metamaterials geometries," *Building Radio Frequency Identification for the Global Environment*, July 2007, [Online], www.bridge-project.eu.
- Eleftheriades, G. V. & Balmain, K. G. (2005) *Negative-Refractive Metamaterials: Fundamentals Principles and Applications*, John Wiley and Sons, Hoboken, New Jersey.
- Finkenzeller, K. (2003). *RFID Handbook: Fundamentals and Applications in Contactless Smart Cards and Identification*, John Wiley and Sons, West Sussex, England.
- Ghadarghad, S.; Ahmadi, A. & Mosellaei, H., "Negative permeability-based electrically small antennas," *IEEE Antennas and Wireless Propagation Letters*, vol. 7, pp. 13-17, 2008.

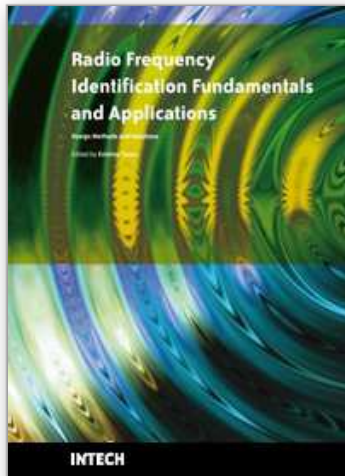
- Gil, M.; Bonache, J.; Selga, J.; Garcia-Garcia, J. & Martin, F. , "Broadband resonant-type metamaterial transmission lines," *IEEE Microwave and Wireless Components Letters*, vol. 17, no. 2, February, 2007, pp. 97-99.
- Herraiz-Martinez, F. J.; Hall, P. S.; Liu, Q. & Sogovia-Vargas, D., "Tunable left-handed monopole and loop antennas," *IEEE Antennas and Propagation Society International Symposium*, July, 2009, Charleston, SC.
- Iizuka, H. & Hall, P.S., "Left-handed dipole antennas and their implementations," *IEEE Transactions on Antennas and Propagation*, vol. 55, no. 5, May, 2007, pp. 1246-1253.
- Lee, C.-J.; Leong, K. M. K. H. & Itoh, T. "Design of resonant small antenna using composite right/left-handed transmission line," *IEEE Antennas and Propagation Society International Symposium*, July, 2005, pp. 218-221.
- Lee, C.-J.; Leong, K. M. K. H. & Itoh, T. "Composite right/left-handed transmission line based compact resonant antenna for RF module integration," *IEEE Transactions on Antennas and Propagation*, vol. 54, no. 8, August, 2006, pp. 2283-2291.
- Mao, S.-G.; Chueh Y.-Z. & Wu, M.-S., "Asymmetric dual-passband coplanar waveguide filters using periodic composite right/left-handed and quarter-wavelength stubs," *IEEE Microwave and Wireless Components Letters*, vol. 17, no. 6, June, 2007, pp. 418-420.
- Marques, R.; Martin, F. & Sorolla, M. (2008). *Metamaterials with Negative Parameters: Theory, Design and Microwave Applications*, John Wiley and Sons, Inc., Hoboken, New Jersey.
- Marrocco, G., "Gain-optimized self-resonant meander line antennas for RFID applications," *IEEE Antennas and Wireless Propagation Letters*, vol. 2, pp. 302-305, 2003.
- Mishra, D.; Poddar, D. R. & Mishra, R. K. "Deformed omega array as LHM," *Proceedings of the International Conference on Recent Advances in Microwave Theory and Applications*, pp. 159-160, Jaipur, India, November, 2008.
- Pozar, D. M. (2005). *Microwave Engineering*, 3rd Ed., John Wiley and Sons, Inc., Hoboken, New Jersey.
- Rao, K. V. S.; Nikitin, P. V. & Lam, S. F., "Antenna design for UHF RFID tags: a review and a practical application," *IEEE Transactions on Antennas and Propagation*, vol. 53, no. 12, pp. 3870-3876, December, 2005.
- Rao, K. V. S.; Nikitin, P. V. & Lazar, S., "An overview of near field UHF RFID" *IEEE International Conference on RFID*, pp. 174-176, March, 2007.
- Ryu, Y.-H.; Lee, J.-H.; Kim, J.-Y. & Tae, H.-S., "DGS dual composite right/left handed transmission lines," *IEEE Microwave and Wireless Components Letters*, vol. 18, no. 7, July, 2008, pp. 434-436.
- Stupf, M.; Mittra, R.; Yeo, J. & Mosig, J. R., "Some novel design for RFID antenna and their performance enhancement with metamaterials," *Microwave and Optical Technology Letters*, vol. 49, no. 4, February, 2007, pp. 858-867.
- Stutzman, W.L. & Thiele, G.A. (1998). *Antenna Theory and Design*, 2nd ed., John Wiley and Sons, Inc., New York.

Vaselaar, D., "Passive UHF RFID design and utilization in the livestock industry," Masters Paper, North Dakota State University, Fargo, ND, 2008.

Ziolkowski, R. W. & Lin, C.-C., "Metamaterial-inspired magnetic-based UHF and VHF antennas," *IEEE Antennas and Propagation Society International Symposium*, July, 2008, San Diego, CA.

IntechOpen

IntechOpen



Radio Frequency Identification Fundamentals and Applications Design Methods and Solutions

Edited by Cristina Turcu

ISBN 978-953-7619-72-5

Hard cover, 324 pages

Publisher InTech

Published online 01, February, 2010

Published in print edition February, 2010

This book, entitled Radio Frequency Identification Fundamentals and Applications, Bringing Research to Practice, bridges the gap between theory and practice and brings together a variety of research results and practical solutions in the field of RFID. The book is a rich collection of articles written by people from all over the world: teachers, researchers, engineers, and technical people with strong background in the RFID area. Developed as a source of information on RFID technology, the book addresses a wide audience including designers for RFID systems, researchers, students and anyone who would like to learn about this field. At this point I would like to express my thanks to all scientists who were kind enough to contribute to the success of this project by presenting numerous technical studies and research results. However, we couldn't have published this book without the effort of InTech team. I wish to extend my most sincere gratitude to InTech publishing house for continuing to publish new, interesting and valuable books for all of us.

How to reference

In order to correctly reference this scholarly work, feel free to copy and paste the following:

Benjamin D. Braaten and Robert P. Scheeler (2010). Design of Passive UHF RFID Tag Antennas Using Metamaterial-Based Structures and Techniques, Radio Frequency Identification Fundamentals and Applications Design Methods and Solutions, Cristina Turcu (Ed.), ISBN: 978-953-7619-72-5, InTech, Available from: <http://www.intechopen.com/books/radio-frequency-identification-fundamentals-and-applications-design-methods-and-solutions/design-of-passive-uhf-rfid-tag-antennas-using-metamaterial-based-structures-and-techniques>

INTECH
open science | open minds

InTech Europe

University Campus STeP Ri
Slavka Krautzeka 83/A
51000 Rijeka, Croatia
Phone: +385 (51) 770 447
Fax: +385 (51) 686 166
www.intechopen.com

InTech China

Unit 405, Office Block, Hotel Equatorial Shanghai
No.65, Yan An Road (West), Shanghai, 200040, China
中国上海市延安西路65号上海国际贵都大饭店办公楼405单元
Phone: +86-21-62489820
Fax: +86-21-62489821

© 2010 The Author(s). Licensee IntechOpen. This chapter is distributed under the terms of the [Creative Commons Attribution-NonCommercial-ShareAlike-3.0 License](#), which permits use, distribution and reproduction for non-commercial purposes, provided the original is properly cited and derivative works building on this content are distributed under the same license.

IntechOpen

IntechOpen